LETTER

Synchronous growth of 30°-twisted bilayer graphene domains with millimeter scale

To cite this article: Jingbo Liu *et al* 2021 *2D Mater.* **8** 021002

View the article online for updates and enhancements.

2D Materials

Synchronous growth of 30°-twisted bilayer graphene domains with millimeter scale

Jingbo Liu[1,2,4,7] (iD), Zegao Wang[2,3,7] (iD), Dongxiong Ling[1], Dongshan Wei[1], Wei Lv[1], Xiaojiao Kang[1], Fei Qi[1,2], Shujiang Ding[4] (iD), Xin Hao[5], Pingjian Li[2] (iD) and Yuanfu Chen[2,6] (iD)

1   School of Electrical Engineering and Intelligentization, Dongguan University of Technology, Dongguan 523808, People's Republic of China
2   State Key Laboratory of Electronic Thin Films and Integrated Devices, University of Electronic Science and Technology of China, Chengdu 610054, People's Republic of China
3   College of Materials Science and Engineering, Sichuan University, Chengdu 610065, People's Republic of China
4   State Key Lab Elect Insulat & Power Equipment, School of Science, Xi'An Jiao Tong University, Xian 710049, People's Republic of China
5   Norla Institute of Technical Physics, Chengdu 610000, People's Republic of China
6   Department of Physics, School of Science, Tibet University, Lhasa 850000, People's Republic of China
7   Jingbo Liu and Zegao Wang contributed equally to this work.

E-mail: lingdx@dgut.edu.cn and yfchen@uestc.edu.cn

Abstract

Bilayer graphene (BLG) with 30°-twist (30°-tBLG) has been proven to possess a quasicrystal structure potentially providing novel applications. Despite the growth of BLG, especially the AB-stacking bilayer, has gained great attention, the growth of 30°-tBLG has been rarely achieved. Herein, for the first time, the decaborane-assisted synchronous growth of millimeter-sized single-crystalline 30°-tBLG was achieved on Cu foil by controlling the nucleation density and growth kinetics of graphene during chemical vapor deposition using diluted methane gas as the carbon source. The synchronous growth kinetics and decaborane-assisted co-catalysis mechanism are revealed by monitoring the growth process from the initial stage of graphene seeds to the millimeter-size scale. A 30°-tBLG based field effect transistor was fabricated and was found to possess a field-effect carrier mobility as high as 3671.3 cm^2 V^{-1} s^{-1} at room temperature. Thus, this work provides a new strategy to grow high-quality and large-scale 30°-tBLG domains which will facilitate their application in the quasicrystal field.

1. Introduction

Compared with monolayer graphene (MLG), bilayer graphene (BLG) has also gained wide attention, where the interlayer rotation provides one more free random to tune its electronic structure enabling unique properties, such as tunable optical excitations, quantum spin Hall effect, superconductivity, interlayer exciton states, the influence of spin–orbit coupling on energy band structure [1–5]. Although the BLG with different rotation exhibits many excellent properties, its controllable large-scale growth is still a great challenge [6, 7].

BLG with AB-stacking exhibited promising application in electronics and optoelectronics, as it has been proved that its band gap can be opened as large as approximately 250 meV by vertical electrical field [8–10]. Although the size of single crystal AB-stacking BLG has already reached millimeter scale, the research on the growth mechanism of BLG with different rotation angle is still a challenge. BLG with 30°-twist (30°-tBLG) has been shown to possess a unique quasicrystal with 12-fold rotational symmetry and exotic quantum phenomenon [11–14]. Recently, there are some methods which have been successfully proposed to synthesize 30°-tBLG on SiC surface [15], Pt substrate [11], Cu–Ni alloy [16], and Cu foil [17]. However, the domain with size as small as micrometers and heterogeneous 30°-tBLG structure both limit its further application. Therefore, it is still a great challenge to synthesize high-quality and large-area 30°-tBLG domains on Cu foil.

The layer-by-layer growth model is the main growth mechanism of graphene on Cu foil, but it is also a limiting factor for the growth of tBLG [18]. BLG domains usually show two common structural forms: wedding cake (on-top growth) and inverted wedding cake (underneath growth). For the wedding cake growth, graphene grows layer-by-layer from the top of the lower layer, while the upper layer grows more slowly, but both of layers have the same nucleus [19, 20]. In contrast, regarding to the inverted wedding cake growth, the bottom layer graphene grows more slowly due to the lack of active carbon atoms that diffusing from the graphene edges, permeating through the existed top layer graphene, or dissolving out from the substrate [21, 22]. The size and shape of the top and bottom graphene layers are diverse due to different growth rates of the two layers. The graphene growth mechanism of the layer-by-layer growth mode remains a controversial topic that must be explored further and has garnered the attention of scientists worldwide. In addition to the on-top growth and underneath growth mechanisms, a synchronous growth mechanism has been proposed recently to expand the understanding of the existing graphene growth mechanisms. Liu *et al* suggested a synchronous growth mechanism of growing BLG on Cu foil, that is, the edge of the top layer graphene is passivated by accurately controlling the hydrogen pressure, so as to promote the formation of nucleation of the bottom graphene [23]. Moreover, using solid polystyrene powder as carbon source, a unique growth process was demonstrated to grow graphene thin films from hexagonal synchronous single crystal domains to wafer-scale uniform thin films [24].

In this study, a simple chemical vapor deposition (CVD) method was proposed to synthesize synchronous large-area 30°-tBLG domains on Cu foil. Its growth process was similar to that of MLG domains, except that decaborane was spin-coated on Cu foil before growth. The tBLG domain is investigated in detail by a variety of material characterization methods and electrical transport measurements. It shows that the tBLG is composed of high quality millimeter-sized single crystal graphene with 30° stacking order. With the assistance of decaborane, the top and bottom layers can grow at almost the same speed at the same time. This research may be beneficial not only to provide a convenient synchronous CVD growth approach of the tBLG domain but also helpful to fundamentally understand the synchronous growth mechanism of BLG on Cu foil.

2. Experimental section

2.1. Synthesis of twisted tBLG domain
By introducing decaborane as co-catalyst, twisted BLG domains were synthesized by a facile CVD process with a gas mixture of Ar, H_2 and diluted CH_4 (200 p.p.m. methane balanced in Ar). Firstly, the 25 μm-thick Cu foil (99.8%, Alfa Aesar) was washed in HCL/H_2O solution (1:10), washed with deionized water (desalted water) for several times to remove the remaining acidic solution, and dried with N_2. Secondly, for decaborane ($B_{10}H_{14}$, 0.03 g ml^{-1} in anisole solution), which was employed as the cocatalyst, spin coating on Cu foil at 3000 rpm for 30 s is very important for the formation of tBLG domains. Thirdly, the Cu foil was loaded into the quartz tube of the CVD system, and then, the growth chamber was heated to 1050 °C with 100 sccm Ar and held for 20 min. Next, the gas mixture of Ar (100 sccm), H_2 (100 sccm) and diluted CH_4 (25 sccm) was introduced into the tube for graphene growth for different times at 1050 °C. Finally, when the CVD system was cooled to room temperature at a cooling rate of 50 °C min^{-1}, the gas mixture flow was closed. For comparison, MLG domains were synthesized by the same method as above, but decaborane was not spin-coated on Cu foil.

2.2. Transfer process of tBLG domain
The transfer of tBLG onto 285 nm SiO_2 substrate was realized by wet etching of Cu substrate. Firstly, the graphene/Cu surface was spin-coated with polymethyl methacrylate (PMMA, A4) at a speed of 3000 rpm for 30 s. Then, overnight, the Cu foil was etched away in ferric chloride solution. Secondly, the PMMA/graphene was washed with deionized water for ten times, then transferred to $H_2O/HCl/H_2O_2$ (20:1:1) solution and $H_2O/NH_4OH/H_2O_2$ (20:1:1) solution for 15 min to remove residual Cu particles and insoluble organic pollutants, respectively. Note that in order to remove the residual solution after each cleaning step, the PMMA/graphene was rinsed with deionized water. Thirdly, the PMMA/graphene was transferred to the SiO_2/Si substrate and cured at 120 °C for 20 min after natural drying, and then the PMMA was removed with acetone and ethanol [25, 26]. For high-resolution transmission electron microscope (HRTEM) characterization, the individual tBLG domain was transferred to the TEM grid with a similar method.

2.3. Characterization
The optical transmittance was measured by using a Perkin–Elmer model Lambda 750 UV–vis–NIR spectrophotometer. Renishaw InVia Raman microscope with 514 nm laser beam was used to collect the Raman spectrum of the tBLG domain. SEM (JSM-7000F) was employed to observe the morphology of the prepared tBLG. X-ray photoelectron spectroscopy (XPS, Kratos XSAM800) was emploed to check the chemical composition of the tBLG. A FEI Tecnai G2 microscope was used to take HRTEM images and selected area electron diffraction (SAED) patterns.
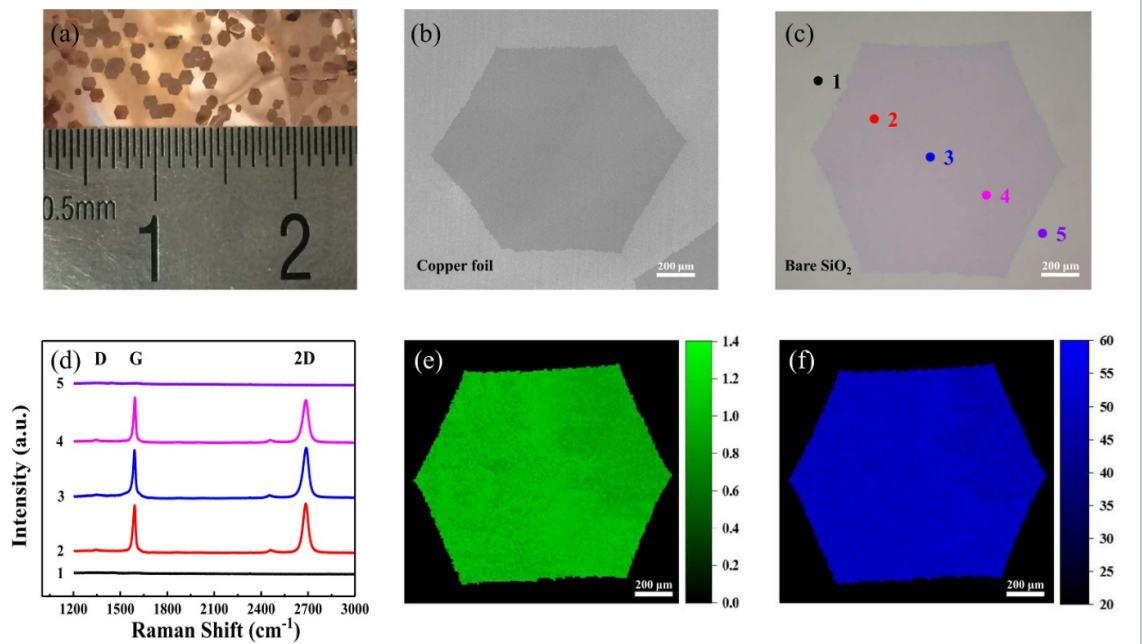
Figure 1. (a) Optical photograph of the tBLG domains grown on Cu foil. (b) SEM image of typical tBLG domain on the Cu foil. (c) The optical image of the graphene domain transferred to SiO$_2$/Si substrate. (d) Raman spectra of the five points marked in (c). (e) I_G/I_{2D} and (f) FWHM of 2D peak Raman mapping of a typical graphene domain on the scale of 1500×1500 μm^2.

2.4. Device fabrication

Field effect transistors (FETs) with back-gated and dual-gated structures were fabricated on conductive Si substrate with 285 nm-thick SiO$_2$ layer. Firstly, the tBLG domain was transferred onto the SiO$_2$/Si substrate. After that, the tBLG domain was patterned into 4 μm wide strips by photolithography and oxygen plasma etching. Then, use photolithography and electron beam evaporation (4 μm width and 40 μm length for back-gated FET) to define and deposit the source and drain electrodes (Ni/Au: 50/50 nm). The Al$_2$O$_3$ film was grown by atomic layer deposition on tBLG domain and work as the to-gated dielectric layer. Finally, the device was annealed with H$_2$/Ar (100/100 sccm) at 250 °C for 2 h.

3. Results and discussion

3.1. Bilayer graphene characterization

Figures 1(a) and (b) show the photograph of multiple graphene domains and SEM image of a random graphene domain on the Cu foil, respectively, which exhibit a distinct hexagon shape with a domain size of ~1200 μm. The clear uniform contrast indicates that there are no different scale layers. To examine the yield of large scale tBLG, the size histogram of over 50 random domains is shown in figure S1 (available online at stacks.iop.org/2DM/8/021002/mmedia). As seen, the tBLG domain with size over 800 μm and 1000 μm are 91% and 77%, respectively, which is significantly larger than the previously reported value of 100 μm scale [16, 17]. Its homogeneity need further optimized. Figure 1(c) shows the visual image

of the graphene domain that was transferred to the SiO$_2$/Si substrate. Raman spectroscopy, as an effective method for determining the number of graphene layers, is employed to characterize the five points marked in figure 1(c) [27, 28]. There is no obvious signal at point 1 and point 5 as shown in figure 1(d), indicating that there is no graphene formed out of the domain. Moreover, the corresponding color differences also confirm the same conclusion. The corresponding Raman spectra of graphene domain from point 2 to point 4 shown in figure 1(d), the typical G band and 2D band are observed at 1591 and 2689 cm^{-1}, respectively. As seen, the D band locating at 1350 cm^{-1} is close to the limit of detection of Raman spectroscopy at point 2 to point 4. The ratios of I_D/I_G are all below 0.1 suggesting its high quality. The peak density ratio of G to 2D (I_G/I_{2D}) is ~0.7, and the full width at half maximum (FWHM) of the 2D peak is ~46 cm^{-1}, indicating that the graphene domain is BLG. Raman mapping of the I_G/I_{2D} and FWHM of the 2D peak on the 1500×1500 μm^2 scale of a random graphene domain are shown in figures 1(e) and (f), respectively. The I_G/I_{2D} ratios of more than 99% graphene region are in the range of 0.7–1.4, and the FWHM values of 2D peak are in the range of 45–60 cm^{-1} (as shown in figure S2), indicating the high uniformity of the prepared BLG domain. There is no obvious boundary between the bottom graphene and the top graphene, indicating that both the top and bottom layers grow simultaneously from the same graphene nuclei with the same growth rate. Furthermore, the thickness of tBLG was further confirmed by measuring the optical transmittance. The
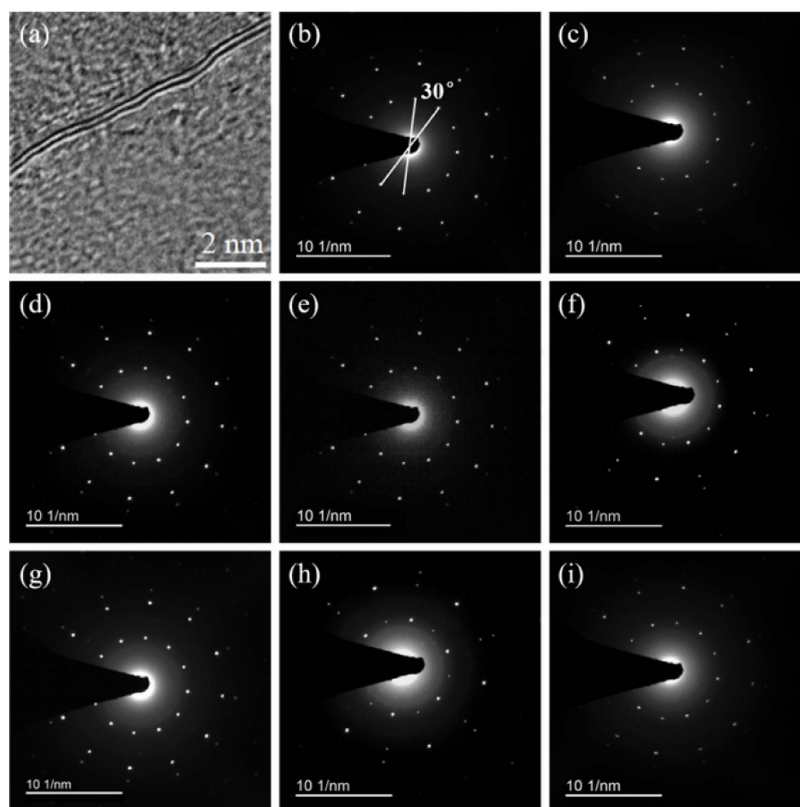
Figure 2. (a) High-resolution TEM image of the random edge of tBLG domain on a TEM grid. (b)–(i) SAED patterns taken from eight random regions at almost the same rotation angle of 30° from the single tBLG domain.

optical transmittance as a function of wavelength of MLG and tBLG on quartz substrate was shown in figure S3. From figure S3, the transmittance of tBLG is 94.74%, which is 2.63% smaller than that of MLG (97.37%) at 550 nm, as similar to previous reports [25].

In order to further verify the number of layers and stacking order of the graphene domain, the structure of BLG domain was characterized by TEM [9, 29]. Figure 2(a) shows an illustration of the random edge of the suspended graphene domain, which unequivocally confirms the bilayer structure of the BLG domain. Eight random SAED patterns have been obtained as shown in figures 2(b)–(i), and all reveal two sets of six-fold symmetry diffraction spots of carbon atoms with almost the same rotation angle of 30° in different regions in the same graphene domain, thus indicating a quasicrystal at the tested location. TEM measurement results show that the synthesized graphene domain is 30°-tBLG domain which is similar with previous reports [14, 17].

3.2. Growth mechanism of bilayer graphene
Decaborane was considered as a catalyst for methane molecular decomposition on Cu foil during the tBLG domain growth process. To gain further insight into the involvement of decaborane, the catalytic effect of decaborane was studied by XPS measurement. Figure 3(a) shows that there is a weak B peak,

which is consistent with that of the decaborane powder, indicating that weak B1s peak originates from the tBLG domain or the remaining decaborane on the Cu foil substrate. In addition, after transferring the tBLG domain to the SiO$_2$/Si substrate, the B1s XPS signal becomes below the detection limit, which means that the rest of the decaborane originated from the Cu foil substrate, not the tBLG domain. This demonstrates that decaborane diffuses into the Cu foil substrate rather than doping into the tBLG domain lattice. To further substantiate the catalytic role of decaborane, as a comparative study, the MLG domain was synthesized with the same growth parameter of tBLG domain, but decaborane was spin coated onto Cu foil before growth. The similar size (∼1200 mm) of the MLG domain to tBLG domain is observed, as shown in figure 3(b). It suggests that the spin-coated decaborane would not affect the scale of the graphene domain. The synthesized graphene domain with monolayer structure is characterized by typical Raman spectrum and HRTEM which are shown in figures 3(c) and (d), respectively. The values of I_G/I_{2D} and 2D peak FWHM of the as-synthesized MLG domain are ∼0.36 and ∼40 cm^{-1}, indicating a monolayer structure. The clear boundary of graphene domain in HRTEM image also demonstrates that the grown graphene is monolayer. This indicates that decaborane is the most critical factor for the growth of tBLG domain.
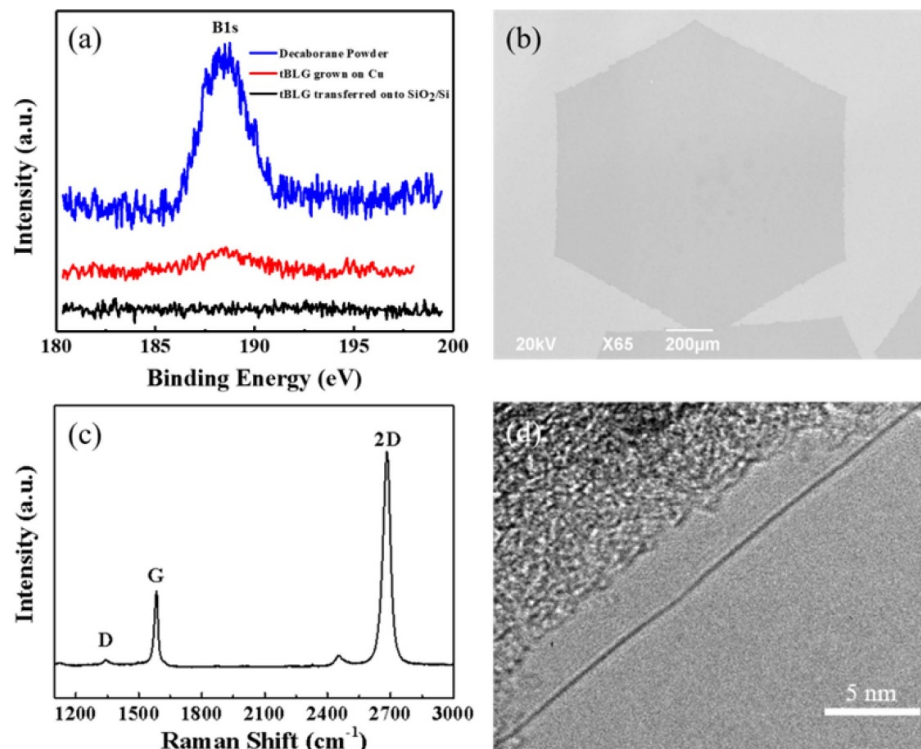
Figure 3. (a) The B1s spectrum of the decaborane powder, the tBLG domain on Cu foil and the tBLG domain transferred to the SiO$_2$/Si substrate, respectively. (b) SEM image of MLG domain grown without decaborane. (c) Typical Raman spectrum and (d) HRTEM of as-synthesized MLG domain.

Therefore, the above studies confirmed that decaborane did not react with tBLG domain or Cu foil, but only played the catalytic role in decomposing methane molecules on Cu foil during the growth of tBLG domain.

In order to further understand the growth mechanism of the tBLG domain and monitor the intermediate growth states, the effect of growth time (from 30 min to 720 min) on different growth stages were studied. During the initial growth process, by setting the growth time at 30 min, as shown in the SEM image of figure 4(a), the symmetrical hexagonal graphene seed was formed on the Cu foil with the size of approximately 75 μm. There is no obvious chromatic aberration from the edge of the initial graphene seed in the SEM image. This proves that the graphene seed grown by synchronous growth mode from the initial stage of the graphene growth process. Raman spectrum with $I_G/I_{2D} \sim 0.9$ and FWHM of the 2D peak ~ 58 cm^{-1} of the synthesized initial stage hexagonal graphene domain reflects the typical bilayer structure, as shown in figure 4(f) (black line of 30 min). Through the continuous supply of methane, as the growth time increases, the edge of the tBLG domain extends laterally on the Cu surface. By setting the growth time as 360 min, 480 min, 600 min and 720 min, the sizes of the tBLG domains are 820 μm, 1000 μm, 1200 μm and 1300 μm, respectively, as shown in figures 4(b)–(e). From the corresponding Raman spectra of tBLG under different growth

times shown in figure 4(f), the I_G/I_{2D} intensity ratios range from 0.9 to 1.1, and FWHM values of 2D peak range from 50 to 58 cm^{-1}, respectively, indicating BLG. This indicates that with the increase of growth time, the activated carbon atoms are continuously captured by the edge of graphene domain, The size of the graphene field increases accordingly. Further research found that after more than 720 min, the size of the graphene domain did not change significantly. This may be due to the fact that the exposed active Cu catalysts gradually decrease with the increase of the graphene crystal domains, and the dynamic equilibrium is reached between the growth and etching process of the graphene domain, so the size change is no longer obvious. The observed symmetrical regular hexagonal shape graphene domains indicate that the size of tBLG domain increases with the growth time, and the domains maintain the initial thickness. The upper and lower layers of graphene grow at the same growth rate. Therefore, we can conclude that the growth of tBLG is not a layer-by-layer mechanism, and its thickness and stacking sequence are determined at the initial stage of simultaneous growth.

Figure 5 shows a schematic diagram of the proposed synthesis mechanism of tBLG fabricated on Cu foil with the assistance of decaborane. At the initial graphene growth stage, methane molecules are catalyzed and decomposed into activated carbon
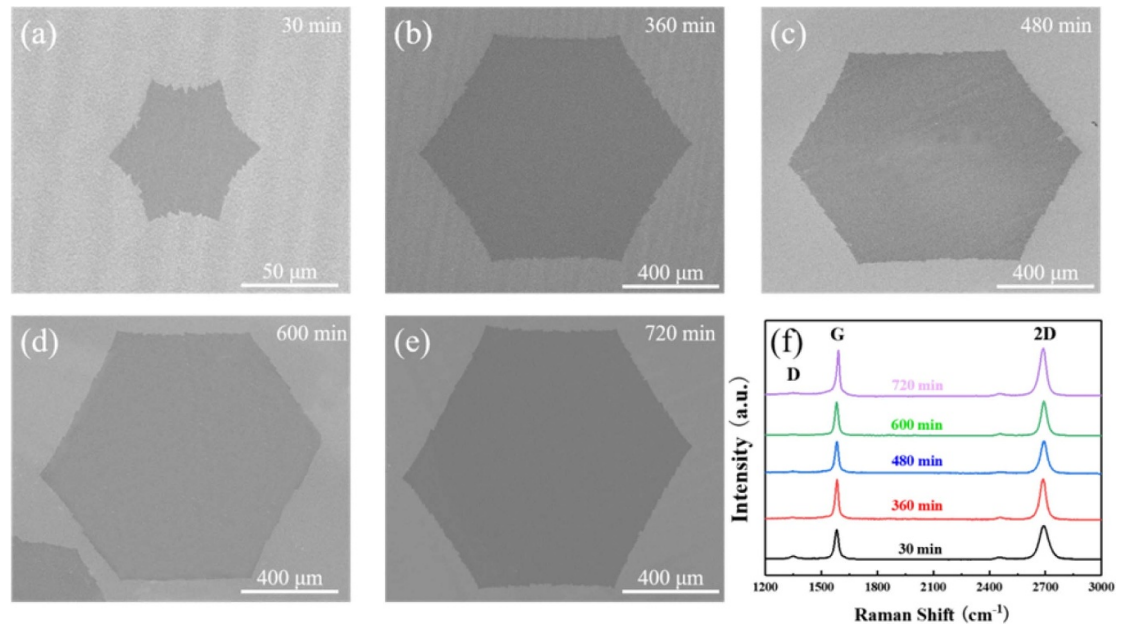
Figure 4. (a)–(e) SEM image of tBLG domain with regular hexagonal shape grown on the Cu foil synthesized with the assistance of decaborane from 30 min to 720 min. (f) Typical Raman spectrum of tBLG domain synthesized from 30 min to 720 min.

atom on the surface of Cu foil by the assistance of hydrogen and decaborane, and subsequently, seeds of tBLG domains are formed. By further increasing the growth time, the size of the tBLG domains laterally grows with the maintenance of their thickness. The graphene seeds grow independently and form tBLG domains before they meet with each other to form a continuous tBLG film or reach the dynamic equilibrium state. This is observed in the experiment during the growth time of 30–720 min. This synchronous growth mechanism is likely to be considered as a process of defining seeding and self-limitation [25]. In view of the fact that the top graphene layer has no direct lateral contact with the Cu foil below, the synchronous growth mechanism is most likely catalyzed by the cocatalytic effect of decaborane close to the graphene domain edges, as shown in illustrations of figure 5. In this way, with the increase of active carbon atoms accumulate at the graphene seed edges, graphene seeds would extend synchronously and grow into graphene domains rather than layer-by-layer. This means that decaborane, as an effective catalyst, would be employed to promote the decomposition of methane at the edge of the tBLG domain. On the other hand, in addition to being the cocatalyst for methane decomposition, decaborane would also hinder the diffusion of active carbon atoms and determine the thickness of graphene layer and the stacking order of graphene domain. Under the auxiliary catalysis of decaborane, the low methane content, which results in the dilution of the active carbon species and the long growth time, promotes large twist angle, especially 30° rotational stacking order, which is different from our previous report [25], to obtain tBLG film with varied twisted

stacking orders under a pure methane concentration growing conditions.

To assess the electrical transport properties of the prepared tBLG domain, back-gated and dual-gated tBLG domain FETs are fabricated on SiO$_2$/Si substrate, and its schematic diagrams are shown in figures 6(a) and (b). The transfer characteristic of the tBLG domain under atmosphere condition of back-gated tBLG transistor is depicted as in figure 6(c). The inset image is the optical microscopy image of tBLG FET on a SiO$_2$/Si substrate. To extract the mobility of the tBLG, the transfer characteristic curve was fitted by equations (1) and (2) [9, 25].

$$R_{\text{total}} = R_{\text{contact}} + R_{\text{channel}} = R_{\text{contact}} + \frac{L}{Wne\mu} \quad (1)$$

$$n = \sqrt{n_0^2 + n_{\text{bg}}^2} = \sqrt{n_0^2 + \left(C_{\text{bg}}\left(V_{\text{bg}} - V_{\text{Dirac}}\right)/e\right)^2}. \quad (2)$$

The total resistance (R_{total}) of the FET device consists of the contact resistance (R_{contact}) and the channel resistance (R_{channel}) of tBLG stripe. Consider the suppress of contact resistance on the carrier mobility of 2D system [30], fitting was performed to remove the influence of contact resistance. L (40 μm) and W (4 μm) are the length and width of the channel, respectively; e is the electron charge; μ is the carrier mobility of graphene; n is the carrier concentration in graphene channel, n_0 is the carrier density at Dirac point, n_{bg} is the carrier density modulated by bottom gate, and C_{bg} (11.5 nF cm^{-2}) is the bottom gate capacitance. In order to extract the carrier mobility, we define
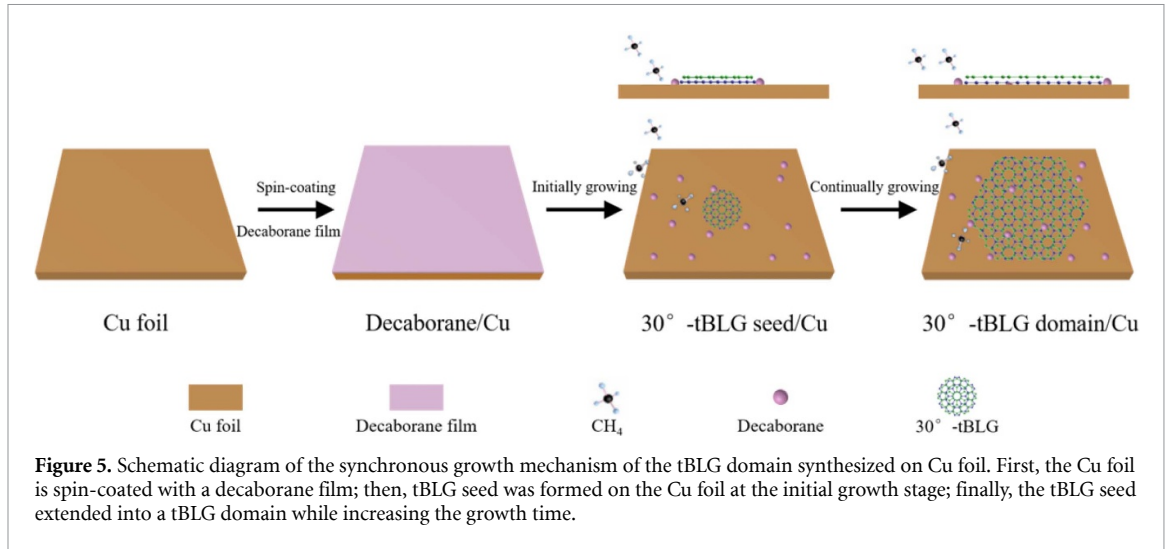
Figure 5. Schematic diagram of the synchronous growth mechanism of the tBLG domain synthesized on Cu foil. First, the Cu foil is spin-coated with a decaborane film; then, tBLG seed was formed on the Cu foil at the initial growth stage; finally, the tBLG seed extended into a tBLG domain while increasing the growth time.
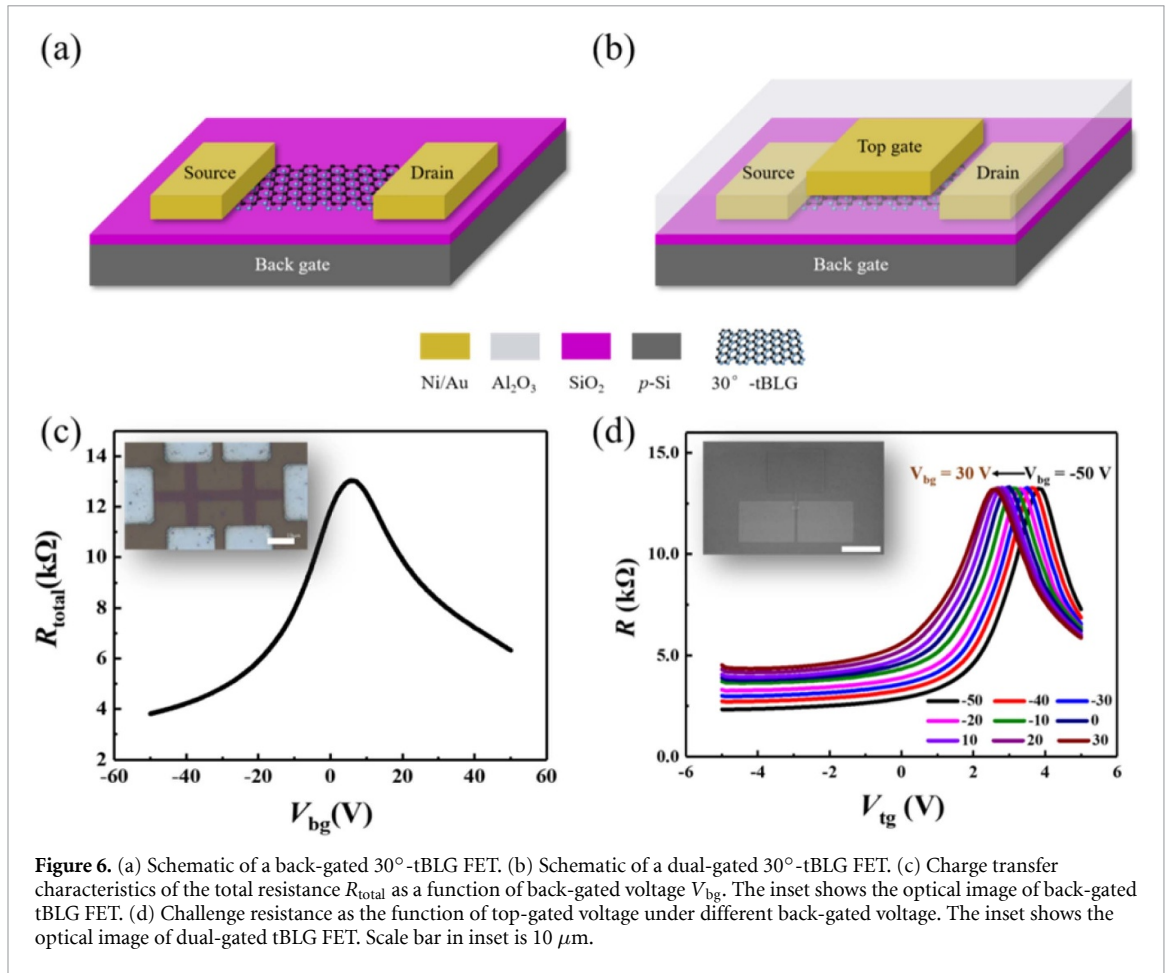

Figure 6. (a) Schematic of a back-gated 30°-tBLG FET. (b) Schematic of a dual-gated 30°-tBLG FET. (c) Charge transfer characteristics of the total resistance R_{total} as a function of back-gated voltage V_{bg}. The inset shows the optical image of back-gated tBLG FET. (d) Challenge resistance as the function of top-gated voltage under different back-gated voltage. The inset shows the optical image of dual-gated tBLG FET. Scale bar in inset is 10 μm.

$$y = a + b \times (c + x)^{-1/2} \qquad (3)$$

where $y = R_{total}$; $a = R_{contact}$; $b = \frac{L}{WC_{bg}\mu}$; $c = \frac{n_0^2 \times e^2}{C_{bg}}$; $x = (V_{bg} - V_{Dirac})^2$ to fit the measured data. So the carrier mobility can be obtained by

$$\mu = \frac{L}{WC_{bg}b}. \qquad (4)$$

The fitting hole mobility of tBLG is as high as 3671.3 cm^2 V^{-1} s^{-1}. We believe that the high mobility

of tBLG is due to the large area and few grain boundaries of millimeter-sized synchronous tBLG domain.

Moreover, figure 6(d) shows the the typical channel resistance (R) as the function of top-gate voltage (V_{tg}) under different back-gate voltages (V_{bg}). Under different displacement fields, the resistance peaks at the neutral point (Dirac point) of the charge are approximately the same, and are similar to the behaviors of dual-gated MLG FET. This result indicates

that there is no obvious bandgap in the 30°-tBLG domain under the dual-gated FET on SiO_2/Si substrate at room temperature, which is similar with previous report [31, 32]. Synchronous large single crystal tBLG domain with preeminent electrical quality is significant to understand the electronic structure and for further research of quasicrystal.

4. Conclusions

By introducing decaborane as a cocatalyst for the decomposition of methane molecules, we have developed a novel method that can synthesize high-quality synchronous 30°-tBLG domains at the millimeter level. Both Raman spectroscopy and TEM were conducted to study their synchronous morphology and twisted single-crystal structure. XPS measurements confirm the catalytic characteristics of decaborane in comparison to the growth process of MLG domains without decaborane. Different from the layer-by-layer growth mechanism, under the catalysis of decaborane, the top and bottom layers of the graphene synchronously grow from the initial tBLG seeds to the millimeter-size tBLG domains at the same growth rate. Electrical transport measurements show that the carrier mobility of tBLG domains reaches up to 3671.3 cm^2 V^{-1} s^{-1} at room temperature. The present work is beneficial to fundamentally understand the synchronous growth mechanism and to pave the way to develop further research of quasicrystal with the large single-crystal tBLG domain.

Acknowledgments

Author contributions

All authors listed have made a substantial, direct and intellectual contribution to the work, and approved it for publication.

Conflict of interest

The authors declare that they have no conflict of interest.

ORCID iDs

Jingbo Liu ⓘ https://orcid.org/0000-0003-3675-267X
Zegao Wang ⓘ https://orcid.org/0000-0002-0033-6538
Shujiang Ding ⓘ https://orcid.org/0000-0002-5683-0973
Pingjian Li ⓘ https://orcid.org/0000-0003-1058-7848
Yuanfu Chen ⓘ https://orcid.org/0000-0002-6561-1684

References

[1] Ju L *et al* 2017 Tunable excitons in bilayer graphene *Science* **358** 907
[2] Finocchiaro F, Guinea F and San-Jose P 2017 Quantum spin Hall effect in twisted bilayer graphene *2D Mater.* **4** 25027
[3] Cao Y, Fatemi V, Fang S, Watanabe K, Taniguchi T, Kaxiras E and Jarillo-Herrero P 2018 Unconventional superconductivity in magic-angle graphene superlattices *Nature* **556** 43
[4] Patel H, Huang L, Kim C-J, Park J and Graham M W 2019 Stacking angle-tunable photoluminescence from interlayer exciton states in twisted bilayer graphene *Nat. Commun.* **10** 1
[5] Wang D, Che S, Cao G, Lyu R, Watanabe K, Taniguchi T, Lau C N and Bockrath M 2019 Quantum Hall effect measurement of spin–orbit coupling strengths in ultraclean bilayer graphene/WSe$_2$ heterostructures *Nano Lett.* **19** 7028
[6] Kerelsky A *et al* 2019 Maximized electron interactions at the magic angle in twisted bilayer graphene *Nature* **572** 95
[7] Culchac F J, Del Grande R R, Capaz R B, Chico L and Morell E S 2020 Flat bands and gaps in twisted double bilayer graphene *Nanoscale* **12** 5014
[8] Zhang Y, Tang T-T, Girit C, Hao Z, Martin M C, Zettl A, Crommie M F, Shen Y R and Wang F 2009 Direct observation of a widely tunable bandgap in bilayer graphene *Nature* **459** 820
[9] Liu L, Zhou H, Cheng R, Yu W J, Liu Y, Chen Y, Shaw J, Zhong X, Huang Y and Duan X 2012 High-yield chemical vapor deposition growth of high-quality large-area AB-stacked bilayer graphene *ACS Nano* **6** 8241
[10] Schwierz F 2010 Graphene transistors *Nat. Nanotechnol.* **5** 487
[11] Yao W *et al* 2018 Quasicrystalline 30 twisted bilayer graphene as an incommensurate superlattice with strong interlayer coupling *Proc. Natl Acad. Sci.* **115** 6928
[12] Koren E and Duerig U 2016 Superlubricity in quasicrystalline twisted bilayer graphene *Phys. Rev.* B **93** 201404
[13] Suzuki T *et al* 2019 Ultrafast unbalanced electron distributions in quasicrystalline 30° twisted bilayer graphene *ACS Nano* **13** 11981
[14] Yan C, Ma D-L, Qiao J-B, Zhong H-Y, Yang L, Li S-Y, Fu Z-Q, Zhang Y and He L 2019 Scanning tunneling microscopy study of the quasicrystalline 30° twisted bilayer graphene *2D Mater.* **6** 45041
[15] Ahn S J *et al* 2018 Dirac electrons in a dodecagonal graphene quasicrystal *Science* **361** 782
[16] Gao Z *et al* 2018 Crystalline bilayer graphene with preferential stacking from Ni–Cu gradient alloy *ACS Nano* **12** 2275

[17] Deng B *et al* 2020 Interlayer decoupling in 30° twisted bilayer graphene quasicrystal *ACS Nano* **14** 1656

[18] Qing F, Shen C, Jia R, Zhan L and Li X 2017 Catalytic substrates for graphene growth *MRS Bull.* **42** 819

[19] Yan K, Peng H, Zhou Y, Li H and Liu Z 2011 Formation of bilayer Bernal graphene: layer-by-layer epitaxy via chemical vapor deposition *Nano Lett.* **11** 1106

[20] Han J, Lee J and Yeo J 2016 Large-area layer-by-layer controlled and fully Bernal stacked synthesis of graphene *Carbon* **105** 205

[21] Ta H Q, Perello D J, Duong D L, Han G H, Gorantla S, Nguyen V L, Bachmatiuk A, Rotkin S V, Lee Y H and Rümmeli M H 2016 Stranski–Krastanov and Volmer–Weber CVD growth regimes to control the stacking order in bilayer graphene *Nano Lett.* **16** 6403

[22] Li Q, Chou H, Zhong J-H, Liu J-Y, Dolocan A, Zhang J, Zhou Y, Ruoff R S, Chen S and Cai W 2013 Growth of adlayer graphene on Cu studied by carbon isotope labeling *Nano Lett.* **13** 486

[23] Liu Q, Gong Y, Wilt J S, Sakidja R and Wu J 2015 Synchronous growth of AB-stacked bilayer graphene on Cu by simply controlling hydrogen pressure in CVD process *Carbon* **93** 199

[24] Wu J *et al* 2017 Synchronous growth of high-quality bilayer Bernal graphene: from hexagonal single-crystal domains to wafer-scale homogeneous films *Adv. Funct. Mater.* **27** 1605927

[25] Liu J *et al* 2015 Observation of tunable electrical bandgap in large-area twisted bilayer graphene synthesized by chemical vapor deposition *Sci. Rep.* **5** 15285

[26] Liang X *et al* 2011 Toward clean and crackless transfer of graphene *ACS Nano* **5** 9144

[27] Malard L M, Pimenta M A, Dresselhaus G and Dresselhaus M S 2009 Raman spectroscopy in graphene *Phys. Rep.* **473** 51

[28] Havener R W, Zhuang H, Brown L, Hennig R G and Park J 2012 Angle-resolved Raman imaging of interlayer rotations and interactions in twisted bilayer graphene *Nano Lett.* **12** 3162

[29] Sun Z, Raji A-R O, Zhu Y, Xiang C, Yan Z, Kittrell C, Samuel E L G and Tour J M 2012 Large-area Bernal-stacked Bi-, Tri-, and tetralayer graphene *ACS Nano* **6** 9790

[30] Wang Z, Xiong X, Li J and Dong M 2020 Screening fermi-level pinning effect through van der waals contacts to monolayer MoS$_2$ *Mater. Today Phys.* **16** 100290

[31] Luican A, Li G, Reina A, Kong J, Nair R R, Novoselov K S, Geim A K and Andrei E Y 2011 Single-layer behavior and its breakdown in twisted graphene layers *Phys. Rev. Lett.* **106** 126802

[32] Li J, Martin I, Büttiker M and Morpurgo A F 2010 Topological origin of subgap conductance in insulating bilayer graphene *Nat. Phys.* **7** 38